Diurnal fluctuations in seawater pCO_2 amplify the negative effects of ocean acidification on the biotic performance of the calcifying macroalga *Halimeda opuntia*

Zhangliang Wei[1,2,3], Yating Zhang[1,4], Fangfang Yang[1]*
and Lijuan Long[1,2,3]*

[1]Chinese Academy of Sciences (CAS) Key Laboratory of Tropical Marine Bio-Resources and
Ecology, South China Sea Institute of Oceanology, Chinese Academy of Sciences, Guangzhou,
China, [2]Guangdong Provincial Observation and Research Station for Coastal Upwelling Ecosystem,
South China Sea Institute of Oceanology (SCSIO), Shantou, China, [3]Key Laboratory of Tropical
Marine Biotechnology of Hainan Province, Sanya Institute of Oceanology, South China Sea Institute
of Oceanology (SCSIO), Sanya, China, [4]College of Earth and Planetary Sciences, University of
Chinese Academy of Sciences, Beijing, China

Although the adverse effects of increasing atmospheric CO_2-induced ocean acidification (OA) on marine calcifying macroalgae have been widely reported, there are limited studies on how daily fluctuations in pCO_2 (pH) within shallow ecosystems influence the growth and physiological performance of these calcifiers. Therefore, a 42-day laboratory mimetic experiment to determine how growth, biological performance and related carbon and nitrogen metabolic products of the calcifying macroalga, *Halimeda opuntia* are generated in response to fluctuating pCO_2 under OA conditions (1200 ppmv) was performed. The results of present study showed that the adverse effects of OA were more determined by the adverse influence of elevated acidity (H^+) on growth rates, calcification, photosynthesis and the related biotic performance of *H. opuntia* compared with the positive effects that higher CO_2 provided. Moreover, diurnal fluctuations in pCO_2 levels [with higher (nearly 8.10) and lower pH (nearly 7.40) values during day and night times, respectively] have amplified these negative influences on *H. opuntia*. To mitigate elevated pCO_2-related stress, higher contents of free amino acids and proline were highly

secreted and likely linked to protecting the integrity of algal cellular structures. The above results contribute to increasing our understanding of the biological consequences of $p\text{CO}_2$ (pH) variability on calcifying *Halimeda* species and their physiological plasticity in response to further oceanic $p\text{CO}_2$ changes.

Introduction

Atmospheric CO_2 reached up to 412.15 ± 0.1 ppm in 2020, and preliminary data for 2021 suggest a rebound in CO_2 relative to 2020 of + 4.8% (4.2% to 5.4%) globally, which is thought to be initially and primarily caused by fossil fuel emissions and deforestation (Friedlingstein et al., 2022). The absorption of CO_2 has already caused apparent changes in the carbonate chemistry of surface seawater and is predicted to decrease by 0.44 ± 0.005 units from 1870–1899 to 2080–2099 (Masson-Delmotte et al., 2021), thus, resulting in an ongoing process and this trend called ocean acidification (OA) (Caldeira and Wickett, 2003; Gattuso et al., 2015; Masson-Delmotte et al., 2021). To date, there have been considerable studies on the impacts of OA on marine organisms, especially macroalgae, because they are important marine primary producers. Elevated $p\text{CO}_2$ would benefit the growth and photosynthesis of some autotrophic macroalgae, such as the economically important macroalgae, *Gracilaria lemaneiformis* (Chen et al., 2018), and *Pyropia yezoensis* (Bao et al., 2019), as well as the green macroalga *Ulva lactuca* (Olischläger and Wiencke, 2013) and *U.prolifera* (Gao et al., 2017). In addition, no obvious effects of elevated $p\text{CO}_2$ on *Ulva rigida* have been demonstrated (Rautenberger et al., 2015; Gao et al., 2018). However, downward trends in growth rate and pigment accumulation have been observed in *Pyropia yezoensis* (Mercado et al., 1999) and calcifying macroalgae *Halimeda* spp. (Campbell et al., 2016; Wei et al., 2020a). Egilsdottir et al. (2013) investigated the lower *m*Mg/Ca ratio of calcite and fewer structures in new fragments produced by the red calcareous coralline alga *Corallina elongata* under elevated $p\text{CO}_2$ (550, 750, and 1,000 ppmv) conditions. A similar phenomenon was reported by Ragazzola et al. (2012), who demonstrated that under elevated $p\text{CO}_2$ conditions, the *m*Mg/Ca ratio in the skeletal calcite of the coralline macroalga *Lithothamnion glaciale* was too small to maintain the stability of skeletal structures by higher ecological niche predators and additional energy to withstand bioerosion and physical erosion. These species-specific responses of macroalgae to OA (elevated

$p\text{CO}_2$) might be attributed to the efficiency of dissolved inorganic carbon (CO_2 utilization and/or elevated acidity) (Egilsdottir et al., 2013; Qu et al., 2017; Chen et al., 2018).

The *Halimeda* genus of green calcareous macroalgae (Chlorophyta, Bryopsidales) is an ecologically important carbonate macroalgae that is widely distributed in tropical and sub-tropical reefs and lagoons (Hofmann et al., 2014; Wei et al., 2020a; Wei et al., 2020b; Wei et al., 2020c). On a global scale, carbonate sediment production by *Halimeda* species accounts for nearly 8% of the carbonate budget, at 0.15–0.4 Gt CaCO_3 year^{-1} (Milliman, 1993; Hillis, 2001). Previous studies suggested that CaCO_3 biomineralization in some marine organisms, including *Halimeda* spp., is an enzymatic process that mainly uses bicarbonatefmars.2022.968740, such as the action of a $\text{Ca}^{2+}/\text{H}^+$-ATPase present in the calicoblastic epithelium (Jury et al., 2010; Wizemann et al., 2015). Studies have documented that biotic CaCO_3 precipitation is significantly and adversely affected by the elevation of seawater $p\text{CO}_2$, because the CaCO_3 saturation (Ω) and pH values are consequently reduced. However, moderate elevations in $p\text{CO}_2$ induce a higher HCO_3^- availability, which contributes to calcification and photosynthesis processes (Hofmann et al., 2014; Vogel et al., 2015; Campbell et al., 2016; Wei et al., 2020a). For instance, Yildiz et al. (2013) found that low pH (7.7) increased the relative electron transport rates (rETR) of calcified rhodophyte *Corallina officinalis*. These wide variety of responses by calcifiers is likely due to either taxonomic distinctions (Kroeker et al., 2010; Peach et al., 2017) or the interactive effects of other environmental factors, such as light intensities (Teichberg et al., 2013; Wei et al., 2020a), seawater temperature (Campbell et al., 2016), nutrient regimes (Teichberg et al., 2013) and/or pH fluctuations (Cornwall et al., 2013).

Compared with pelagic oceans, in coastal waters the magnitude of diurnal pH variation always exceeds 0.6 units owing to the CO_2 uptake by photosynthesis during the day time and CO_2 release *via* respiration and other biological activities during the night time. Moreover, the large-scale nutrient inputs from human industry and agriculture have aggravated diurnal pH variations in coastal waters (Egilsdottir

et al., 2013). Qu et al. (2017) demonstrated that under diurnal pH fluctuation conditions, from approximately 7.83 to approximately 8.44, the adverse effects of acidity (H^+) on the photosynthetic performance of the red macroalga *Gracilaria lemaneiformis* cultivated under high-density conditions that resulted from the CO_2 uptake was relatively small. Therefore, the diurnal variability of pH occurring in marine ecosystems is a non-negligible environmental factor affecting the growth and metabolic processes of marine organisms in current oceans and may have characteristic implications for predicting the responses of marine calcifiers to OA in the future (Cornwall et al., 2013). The capacity of marine calcifiers to resist significant diurnal pH/pCO$_2$ fluctuations may be a result of short-term acclimation (due to the phenotypic plasticity of the individual) and/or long-term adaptation (genetic endowment by the population) (Egilsdottir et al., 2013). For instance, Martin and Gattuso (2009) reported that the reduced calcification rate of coralline alga *Lithophyllum cabiochae* was observed under elevated pCO$_2$ conditions after 1 month, but no obvious effects were observed after acclimatization for 1 year. Thus, to accurately predict how climate changes will affect marine organisms, it is essential to preferentially determine the present detailed effects of specific environmental variabilities on marine species at both local and larger regional scales (Cornwall et al., 2013; Reusch and Boyd, 2013).

Halimeda species may be sensitive to highly variable environments. Teichberg et al. (2013) found that photosynthetic pigment concentrations in *Halimeda opuntia* were usually higher in deep than shallow waters to enhance light acquisition in areas having low light conditions, whereas carotenoids play a role in photoprotection for mitigating light stress. These phenomena have also been widely found in macroalgae that grow in tropical shallow waters (Beach et al., 2003). To date, however, there are limited studies on how daily fluctuations in pCO$_2$ (pH) within shallow ecosystems influence the growth and physiological performance of marine calcifiers, including *Halimeda* species. Therefore, the purpose of the present study was to examine how abiotic responses of *Halimeda* to OA are influenced by diurnal fluctuations in seawater pCO$_2$ (pH). It has been hypothesized that (1) periods of relatively lower CO_2/higher pH may ameliorate negative influences of OA on marine calcifiers to some degree, by providing short rest intervals that may be beneficial to their calcification (Hurd et al., 2011; Dufault et al., 2012), or (2) amplify the negative effects of OA on biotic performance owing to the extreme mean decreases in pH, especially during the night (Cornwall et al., 2013). These physiological descriptions of accurately mimicked laboratory incubation experiments will provide a better understanding of the responses of marine calcifying organisms to future global climate change-mediated alterations in pH levels.

Materials and methods

Monitoring *in situ* pH fluctuations and sample collection

For a description of the pH fluctuations at the *Halimeda* community sampling site located in the Xisha Islands, South China Sea (9.53°–9.60° N, 115.34°–115.46° E), pH values were monitored at 6:00 and 18:00 daily for 30 days (June 1 to 30, 2021) using a YSI meter (YSI Professional Plus, Yellow Springs, OH, USA). The average pH values within the *Halimeda* community at 6:00 and 18:00 were 8.43 and 7.63, respectively, indicating that the pH variability ranged by 0.80 units during the *in situ* monitoring period (Figure 1) and contributed to our subsequent experiment design (as described in 2.2). Afterwards, thalli of *H. opuntia* were sampled in a fore reef lagoon at depths ranging from 1.5–2.5 m and then transported back to the laboratory. To acclimatize the macroalgae to the experimental conditions, they were gently rinsed with filtered seawater and maintained in a large mesocosm tank (2, 000 L) that received a constant fresh sandy-filtered seawater (~45 L/min) under controlled conditions (approximately 27°C, 32 PSU, pH ~8.1, and 80 µmol photons m^{-2} s^{-1} with a 12-h: 12-h day: night cycle) for 3 weeks (Hofmann et al., 2014). Irradiance intensities were created using a combination of white FMW39TS and blue FMB5AT5 light bulbs (Arcadia, Redhill, UK) (Wei et al., 2020a). During the acclimation period, *H. opuntia* samples turned healthy green, indicating that subsequent experiments could be undertaken.

Experimental design and treatments

After the monitoring *in situ* pH fluctuations and initial acclimation period, *H. opuntia* individuals were randomly subjected to experimental manipulations of two static pCO$_2$ levels combined with two fluctuating pCO$_2$ levels within aquaria for 42 days (July 1 to August 11, 2021). For each treatment, there were eight algal thalli [110–120 g fresh weight (FW) in total] in one aquarium (30 L), and three biological replications were prepared per treatment. All the individuals were evenly spaced across the bottom of each aquarium to avoid self-shading, and the 0.45-µm-filtered seawater was replaced every 3 days. The pCO$_2$ (OA) was elevated by bubbling pure CO_2 mixed with ambient air automatically into the seawater in each aquarium (CE100C, Wuhan Ruihua Instrument and Equipment Ltd., Wuhan, China). The static elevated pCO$_2$ (OA-ST) was set at 1,200 ppmv, which is the level predicted under extreme conditions by year 2100 (Caldeira and Wickett, 2005). The fluctuations in the elevated pCO$_2$ concentration treatment (OA-FT) were 450
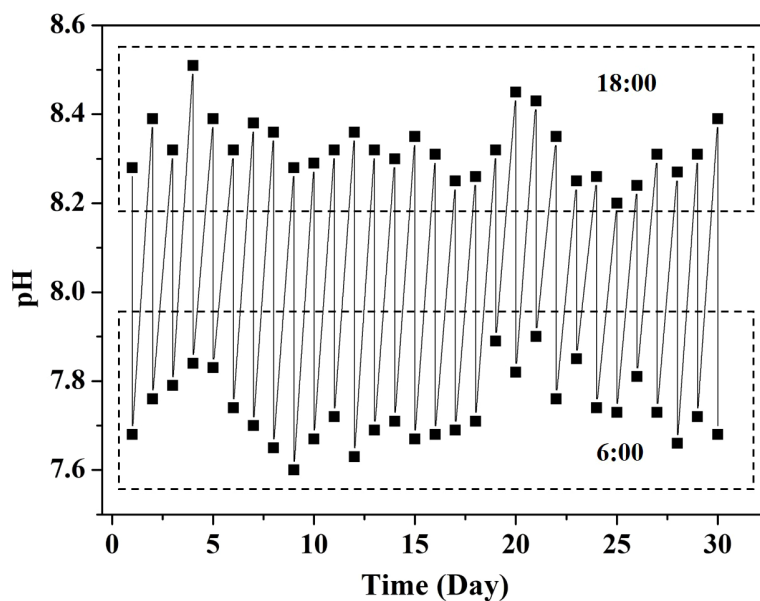
FIGURE 1
The pH measurements at 6:00 and 18:00 daily over 30 days at an average depth of 2.0 m (1.5–2.5 m) from the sampling site located in the South China Sea.

ppmv and 1,800 ppmv during day and night times, respectively. The static ambient pCO$_2$ concentration (AM-ST) was the current local pCO$_2$ level (approximately 450 ppmv), whereas the fluctuation in the ambient pCO$_2$ treatment (AM-FT) during day time was set at 100 ppmv, which was achieved by bubbling post-CO$_2$ mixed with ambient air, and the pCO$_2$ during the night time was set at 1,200 ppmv (Table 1).

Monitoring experimental conditions

To ensure the continuity of the culture conditions among treatments, seawater column chemistry monitoring was conducted daily at the end of the light (18:00) and dark (06:00) periods during the 42-day experiment. Seawater temperature (°C) and salinity (PSU) were determined using a handle YSI meter. The pH$_{NBS}$ valves were obtained using an S220 pH electrode (Thermo Scientific Orion, Waltham, MA, USA) and corrected with standard buffer solution (pH 7 and 10). Total alkalinity (TA) in each aquarium was measured daily using the Gran titration method and corrected by alkalinity reference materials (CRM; Andrew Dickson Lab, Scripps Institute of Oceanography) (Metrohm 877 Titrino Plus, Titrando[®] Metrohm USA, Inc.) (Dickson et al., 2007). Measured seawater parameters (salinity, temperature, pH$_{NBS}$, and TA) were used to calculate the levels of dissolved inorganic carbon components using the Excel program CO2SYS (Pierrot et al., 2006).

TABLE 1   Experimental design of static (ST) and fluctuated (FT) current ambient pCO$_2$ (AM), as well as elevated pCO$_2$ (ocean acidification, OA) levels.

Treatments	pH$_{NBS}$ predicted	pCO$_2$ set (ppmv)
AM-ST	8.10	Daytime: 450 Night-time: 450
AM-FT	8.10 ± 0.40	Daytime: 100 Night-time: 1200
OA-ST	7.70	Daytime: 1200 Night-time: 1200
OA-FT	7.70 ± 0.40	Daytime: 450 Night-time: 1800

Growth and calcification rates

The relative growth rate (RGR, % d^{-1}) of *H. opuntia* was calculated in accordance with the following formula (Wei et al., 2021):

$$RGR = [(lnW_t - lnW_{t-42})/42] \times 100,$$

where W_t and W_{t-42} represent the FWs obtained on the 42nd and 1st days, respectively, and 42 represents the time interval between the two sampling days.

The instantaneous net calcification rates (G_{net}) was estimated using the alkalinity anomaly technique on the 42nd day (Campbell et al., 2016). The algal fragments (5.0 g) were incubated in acrylic transparent bottles (1.0 L) containing filtered seawater under four experimental conditions with an electro-magnetic stirrer. The calculation of G_{net} was based on the changes in TA after an 8-h incubation using the following equation:

$$G_{net} = 0.5p \times (TA_0 - TA_n) \times V/(FW \times t),$$

where G_{net} (µmol CaCO$_3$ g FW^{-1} h^{-1}) represents the net calcification rate of whole thalli *H. opuntia*, p represents the seawater density (1.025 kg L^{-1}), TA_0 and TA_n represent the initial TA and TA after n hours of culture (8 h), V represents the seawater volume (1.0 L), and FW and t represent the algal fresh weight (5.0 g) and incubation time (8 h), respectively. When $G_{net} > 0$, calcification occurs, whereas when $G_{net} < 0$, dissolution in CaCO$_3$ mineralogy occurs.

F_v/F_m and pigment contents

The photosystem II (PSII) maximum quantum yield (F_v/F_m) value of *H. opuntia* was measured by a Diving-PAM II fluorometer (Heinz Walz GmbH, Effeltrich, Germany). After 20 min of dark adaptation, F_v/F_m was obtained using red light as the modulated light (5,000 µmol photons m^{-2} s^{-1}, 0.6 s). Together with photosynthetic performance, 200 mg FW of fragment (n = 3) was sampled and immediately frozen in liquid nitrogen for pigment content measurement. Samples were finely ground in 10 ml 90% acetone and extracted at 4°C for 24 h under dark conditions. Afterwards, the homogenate was centrifuged at 4,000 rpm for 10 min (Eppendorf centrifuge 5810 R, Hamburg, Germany). The pigment contents, including chlorophyll (Chl) *a*, *b* and carotenoid concentrations, were measured using the supernatant, as described by Ritchie (2008).

Measurement of total carbon and total nitrogen contents

The total organic carbon (TC$_{org}$) and total nitrogen (TN) contents (dry weight, % DW) in *Halimeda* tissues subjected to the four treatments were determined at the end of the experiment. The samples (n = 3) were washed five times and then dried to constant weight at 60°C. Afterwards, all the samples were finely ground and determined by a CHN Elemental Analyzer (Flash EA300, Thermo Scientific, Milan, Italy).

Measurement of enzyme activities

Samples (200 mg FW of each, n = 3) used to determine enzymatic activities, external carbonic anhydrase activity (eCAA) and nitrate reductase activity (NRA), were collected at the end of the experiment. The algal fragments were ground in 5.0 mL 20-M veronal buffer (pH 8.3) for eCAA and 0.1 M phosphate buffer (pH 7.5) for NRA. The eCAA and NRA levels in the supernatant were determined using algal enzymatic ELISA Kits (Mlbio, Shanghai, China) following the appropriate manufacturer's instructions. Both enzyme activities were corrected using an optical density (OD) standard curve.

Soluble carbohydrate, malondialdehyde, proline and free amino acids

For the determination of the algal soluble carbohydrate (SC) content, 200 mg FW of each sample was collected and ground in 10 ml filtered seawater. After 10 min of centrifuging (5,000 rpm), the SC level in the supernatant was determined using the phenol–sulfuric acid method (Kochert, 1978). The malondialdehyde (MDA) occurrence was measured because it is a potential indicator of lipid peroxidation encountered after environmental stresses (Wei et al., 2020c). In total, 500 mg FW of algal tissues was sampled and ground in 10 ml of 10% trichloroacetic acid, and then centrifuged at 4, 000 rpm for 10 min. The supernatant was collected and MDA was measured as described by Hodges et al. (1999).

To obtain further insights into the algal physiological regulation after exposure to diurnal fluctuations in seawater *p*CO$_2$, the proline and free amino acids (FAAs) were analyzed for maintaining the photosynthetic system functioning and protecting the membranes from various damages (Wei et al., 2020a). At the end of the experiment, 500 mg FW of algal tissue for proline was weighed and finely ground in 5 ml 3% sulfosalicylic acid. The homogenate was shaking for 10 min under 100°C conditions. After 10 min of centrifugation (3,000 rpm), the proline content was measured in the supernatant as described by Shan et al. (2007). To determine FAAs, 200 mg FW of each sample was ground in 5 ml PBS buffer (pH 7.4), and FAAs was measured in the supernatant of the aqueous extract using an algal FAAs ELISA Kit (Mlbio, Shanghai, China), as described in the manufacturer's instructions.

Statistical analyses

All the data in this study were presented as a triplicate mean ± standard deviation (mean ± SD) (n = 3). The figures were created using Origin 8.0 software (Origin Lab Corp., Northampton, MA, USA). All the statistical analyses were conducted using IBM SPSS Statistics 20 software (SPSS Inc., Chicago, IL, USA). A one-way analysis was conducted to determine the differences among the four treatments. Tukey's Honestly Significant Differences was used to make *post hoc* comparisons (95% confidence level). Differences by different uppercase and lowercase letters in Figure 2–7 were considered to be significant at $P < 0.05$ and extremely significant at $P < 0.01$.

Results

Seawater monitoring

The average pH_{NBS} values in static ambient pCO_2 and elevated pCO_2 were 8.10 ± 0.01 and 7.71 ± 0.01, respectively, regardless of day or night time, whereas the average pH_{NBS} values for the two fluctuating pCO_2 levels were 8.43 ± 0.01 and 7.72 ± 0.02 ($P < 0.01$), respectively, in day time and 8.08 ± 0.01 and 7.42 ± 0.02 ($P < 0.01$), respectively, in night time. Nevertheless, the elevated pCO_2 altered the DIC components and aragonite saturation state (Ω_{Arag}) in seawater ($P < 0.01$). In contrast with static ambient (AM-ST) pCO_2 treatments, the mean CO_2 and HCO_3^- concentrations in static

elevated (OA-ST) pCO_2 treatments increased from 14.6–15.3 µmol kg^{-1} to 39.9–41.5 µmol kg^{-1} and 1,898.7–1,940.8 µmol kg^{-1} to 2,172.2–2,196.0 µmol kg^{-1}, respectively, whereas CO_3^{2-} concentrations decreased from 184.2–185.9 µmol kg^{-1} to 87.4–88.1 µmol kg^{-1} ($P < 0.01$). The average CO_2, HCO_3^- and CO_3^{2-} concentrations in fluctuated ambient (AM-FT) and elevated (OA-FT) pCO_2 treatments differed significantly among treatments, as well as between day and night times ($P < 0.01$) (Table 2). The Ω_{Arag} values were lower in elevated pCO_2 treatments, ranging from 0.72 to 1.44, and the highest Ω_{Arag} values were obtained in AM-FT during the day time (5.47 ± 0.18).

Growth and calcification rates of *H. opuntia*

After 42-day experimental exposure, the elevated pCO_2 and daily fluctuations in the pCO_2 of seawater had significant effects on the growth rate of *H. opuntia* (Figure 2). The highest *RGR* was recorded in AM-ST, at 0.266% ± 0.012% d^{-1}. The *RGR* under elevated pCO_2 conditions decreased by 22.02%–44.57% in contrast with those in AM-ST. Notably, daily fluctuating pCO_2 amplified the negative effects on growth rates at two pCO_2 concentration levels. In addition, the *RGR* values in AM-FT (0.226% ± 0.009% d^{-1}) and OA-ST (0.218% ± 0.011% d^{-1}) were not significantly different ($P > 0.05$) (Figure 2).

The G_{net} differed significantly among the four treatments under both light and dark conditions ($P < 0.05$) (Figure 3).
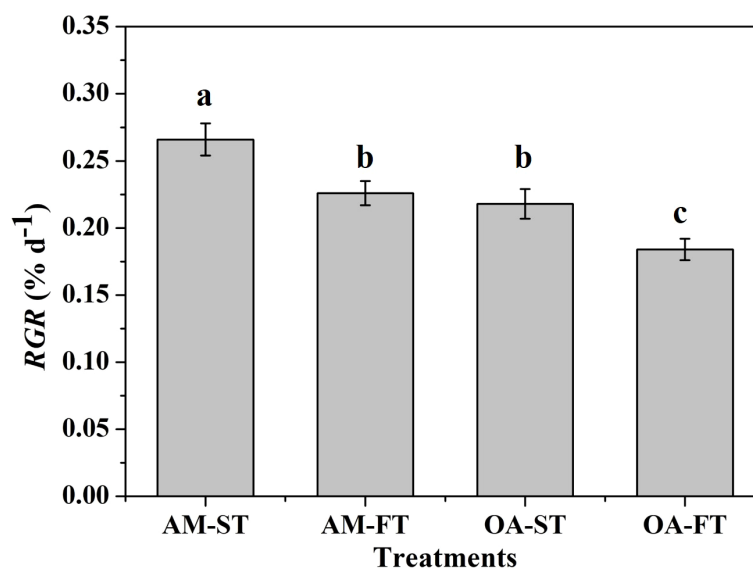

FIGURE 2
The relative growth rates (*RGR*, % d^{-1}) of *Halimeda opuntia* (mean ± SD, n = 3) exposed to the four treatments for 42 days (AM, ambient pCO_2 concentration; OA, ocean acidification; ST, static; FT, fluctuating). Significant differences among the treatments are indicated by different uppercase and lowercase letters, respectively (Tukey's test, P<0.05).

FIGURE 3
The net calcification rates (G_{net}, μmol $CaCO_3$ g FW^{-1} h^{-1}) of *Halimeda opuntia* (mean $\pm$ SD, n = 3) under light and dark conditions after exposure to four pCO_2 treatments for 42 days. Significant differences among the treatments are indicated by different uppercase and lowercase letters, respectively (Tukey's test, P<0.05).
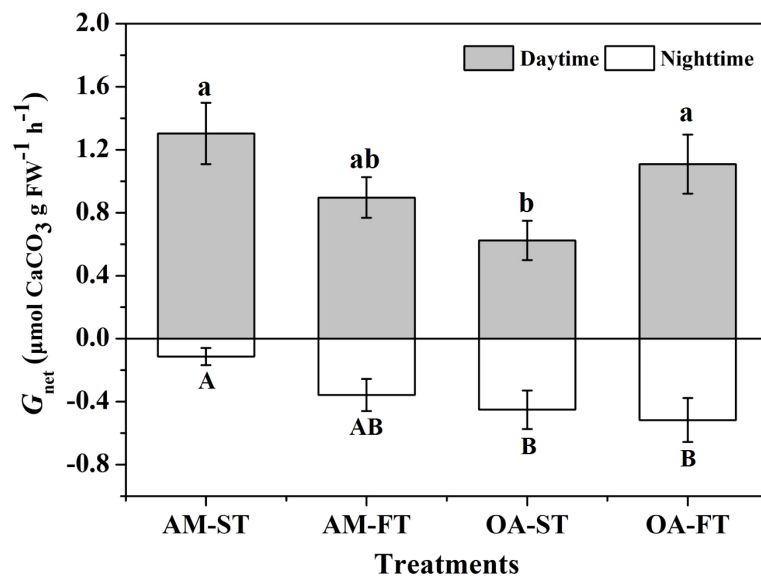
Under light conditions, the greatest net calcification levels occurred in the four treatments. The G_{net} of *H. opuntia* in AM-ST, AM-FT and OA-FT did not change significantly, ranging from 0.897 to 1.303 μmol $CaCO_3$ g FW^{-1} h^{-1} ($P > 0.05$). The lowest G_{net} values were obtained in OA-ST (0.624 $\pm$ 0.124 μmol $CaCO_3$ g FW^{-1} h^{-1}) owing to the elevated pCO_2. Under dark conditions, the greatest net dissolution in $CaCO_3$ mineralogy occurred, as shown in Figure 3. The lowest dissolution rate (–0.114 $\pm$ 0.054 μmol $CaCO_3$ g FW^{-1} h^{-1}) was measured in AM-ST. However, elevated pCO_2 amplified the negative $CaCO_3$ dissolution rate, and the greatest dissolution rate was –0.517 $\pm$ 0.139 μmol $CaCO_3$ g FW^{-1} h^{-1} in OA-FT after dark exposure.

Chlorophyll fluorescence and pigment contents

There were significant direct effects of elevated pCO_2 and daily fluctuating pCO_2 on F_v/F_m and Chl-*a* content ($P < 0.05$). The lowest F_v/F_m was in AM-FT, with a mean value of 0.562 $\pm$ 0.005. Compared with the F_v/F_m (0.630 $\pm$ 0.006) in AM-ST, elevated pCO_2 decreased the F_v/F_m to the 0.614–0.618 range (Figure 4A). Similar to the F_v/F_m variations, the lowest Chl-*a* content was in AM-FT, with a mean value of 175.79 $\pm$ 12.62 μg g^{-1} FW, and there were no obvious Chl-*a* variations in the other three treatments (194.33–225.61 μg g^{-1} FW) (Figure 4B). Across all the treatments, photosynthetic Chl-*b* and carotenoid contents

were not notably influenced, having 134.99–157.49 μg g^{-1} FW and 75.33–87.78 μg g^{-1} FW ranges, respectively (Figures 4C, D).

Tissue total carbon (TC_{org}) and nitrogen (TN) contents
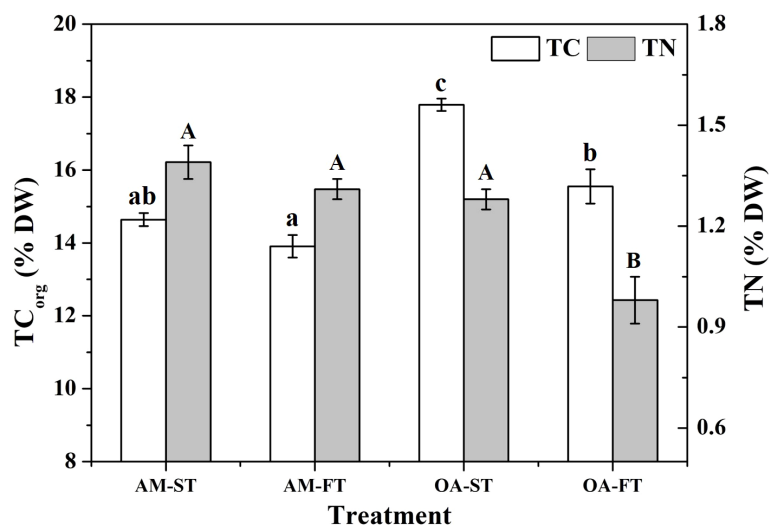
Total organic carbon (TC_{org}) and total nitrogen (TN) in *H. opuntia* tissues were significantly affected by elevated pCO_2 and daily fluctuating pCO_2 ($P < 0.05$) (Figure 5). There were no notable differences between the ambient pCO_2 treatments, regardless of static or fluctuating pCO_2 concentrations ($P > 0.05$). However, an elevated pCO_2 significantly stimulated TC_{org} accumulation by 8.93%–24.62% compared with the average TC_{org} in both AM treatments. The highest TC_{org} content occurred in OA-ST (17.79% $\pm$ 0.77% DW). The TN contents did not significantly vary among the AM-ST, AM-FT and OA-ST treatments (1.28%–1.39% DW) ($P > 0.05$), but it significantly decreased in OA-FT to 0.98% $\pm$ 0.07% DW ($P < 0.01$) (Figure 5).

Enzymatic activities (carbonic anhydrase and nitrate reductase)

There were no obvious effects of static and fluctuating pCO_2 on the eCAA among the four treatments (3.280–3.828 IU mg^{-1} FW) ($P > 0.05$) (Figure 6). Compared with the (NRA in *H. opuntia* tissues incubated under ambient pCO_2 conditions (2.535–2.784 pg
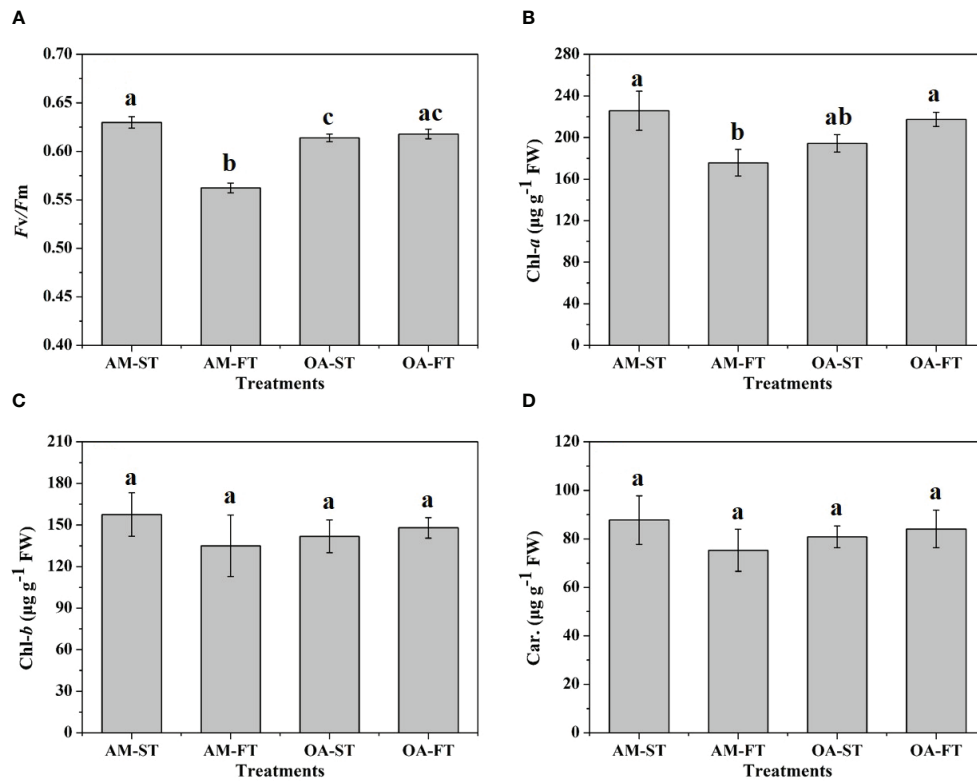
FIGURE 4
Variations in photosynthetic maximum quantum yields (F_v/F_m) **(A)** and in chlorophyll (Chl)*a* **(B)**, *b* **(C)** (µg g^{-1} FW) and carotenoid (Car., µg g^{-1} FW) contents **(D)** of *Halimeda opuntia* (mean ± SD, n = 3) in four pCO$_2$ treatments. Significant differences among the treatments are indicated by different uppercase and lowercase letters, respectively (Tukey's test, P<0.05).

FIGURE 5
Variations in tissue total organic carbon (TC$_{org}$, % DW) and nitrogen (TN, % DW) from the tissues of *Halimeda opuntia* (mean ± SD, n = 3) in four pCO$_2$ treatments. Significant differences among the treatments are indicated by different uppercase and lowercase letters, respectively (Tukey's test, P<0.05).

FIGURE 6
Mean ($\pm$ SD, n = 3) external carbonic anhydrase activity (eCAA, IU mg^{-1} FW) and nitrate reductase activity (NRA, pg mg^{-1} FW) levels in four pCO$_2$ treatments after a 42-day incubation. Significant differences among the treatments are indicated by different uppercase and lowercase letters, respectively (Tukey's test, P<0.05).
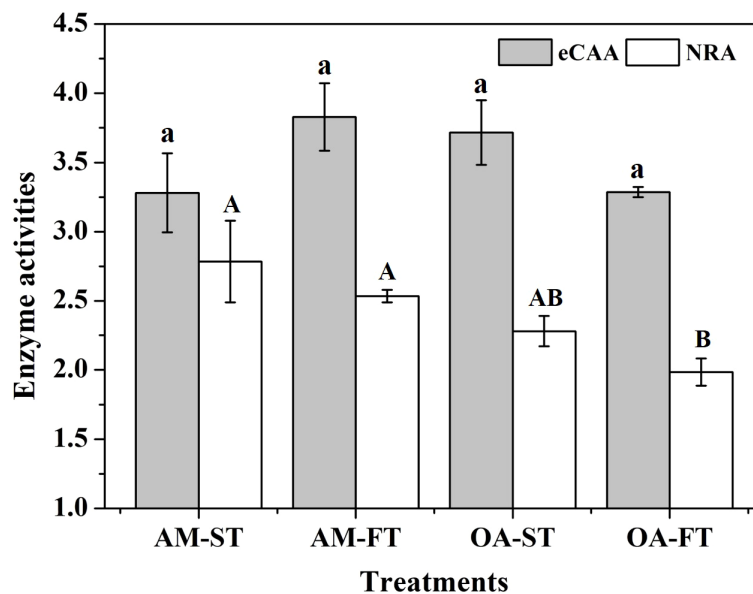
mg^{-1} FW), the NRA decreased under both static and fluctuating elevated pCO$_2$ conditions by 16.63%–34.01%, and the lowest NRA was obtained in OA-FT, having an average value of 1.984 $\pm$ 0.298 pg mg^{-1} FW ($P < 0.05$) (Figure 6).

Soluble carbohydrate, malondialdehyde, proline and free amino acids contents

The soluble cellular compositions were significantly affected by elevated pCO$_2$ and daily fluctuations ($P < 0.01$) (Figure 7). The SC level decreased by 32.38%–67.65% under elevated and fluctuating pCO$_2$ conditions, compared with the SC in AM-ST, and the lowest average SC content occurred in AM-FT at 2.12 $\pm$ 0.01 μg mg^{-1} FW ($P < 0.01$) (Figure 7A). Under elevated pCO$_2$ conditions (OA-ST), the MDA content increased to 2.74 $\pm$ 0.04 μg mg^{-1} FW ($P < 0.01$). Moreover, fluctuating pCO$_2$ amplified the effects of abiotic stress on MDA, which increased to 3.98 $\pm$ 0.05 μg mg^{-1} FW and 3.69 $\pm$ 0.06 μg mg^{-1} FW in AM-FT and OA-FT, respectively (Figure 7B). The proline levels increased notably under elevated and fluctuating pCO$_2$ conditions ($P < 0.01$). The lowest average proline contents was obtained in AM-ST (2.24 $\pm$ 0.06 μg mg^{-1} FW), whereas the highest proline content occurred in OA-FT (4.31 $\pm$ 0.08 μg mg^{-1} FW) (Figure 7C). The FAA content significantly increased in the elevated pCO$_2$ treatment (OA-ST, 3.19 $\pm$ 0.09 μg mg^{-1} FW) compared with in AM-ST (2.50 $\pm$ 0.06 μg mg^{-1} FW). Furthermore, the effects on FAA were enhanced by the two fluctuating pCO$_2$ levels ($P < 0.01$), and the

highest average FAA content occurred in OA-FT (4.46 $\pm$ 0.05 μg mg^{-1} FW) (Figure 7D).

Discussion

The anthropogenic elevation of atmospheric CO$_2$ induced OA, and a lower aragonite saturation (Ω_{Arag}) has been widely reported to negatively affect the growth and calcification processes of marine calcifiers (Campbell et al., 2016; Wei et al., 2020a). Our results demonstrated that the effects of OA were increased by the adverse influence of elevated acidity (H$^+$) on growth rates, calcification, photosynthesis and the related biotic performance of *H. opuntia* compared with the positive effects of a higher CO$_2$ level. Moreover, diurnal fluctuations in pCO$_2$ levels (with a higher pH during the day time and a lower pH during the night time) amplified these negative influences on *H. opuntia*. Similar with our previous study, the growth rates of *Halimeda cylindracea* and *Halimeda lacunalis* decreased significantly by 6.84%–86.70% under elevated pCO$_2$ (1,000–1,600 ppmv) conditions (Wei et al., 2020a). In contrast with non-calcifying macroalgae, such as *G. lemaneiformis* (higher pCO$_2$-grown plants), the increased pCO$_2$ under OA conditions alleviates dissolved carbon limitations and leads to an enhancement in *RGR* (Zou et al., 2004). In this study, *H. opuntia* exhibited negative growth owing to the extremes in the elevated pCO$_2$ variations. Because the photosynthetic rate of this alga has been completely saturated at the present seawater pCO$_2$ (Zou et al.,
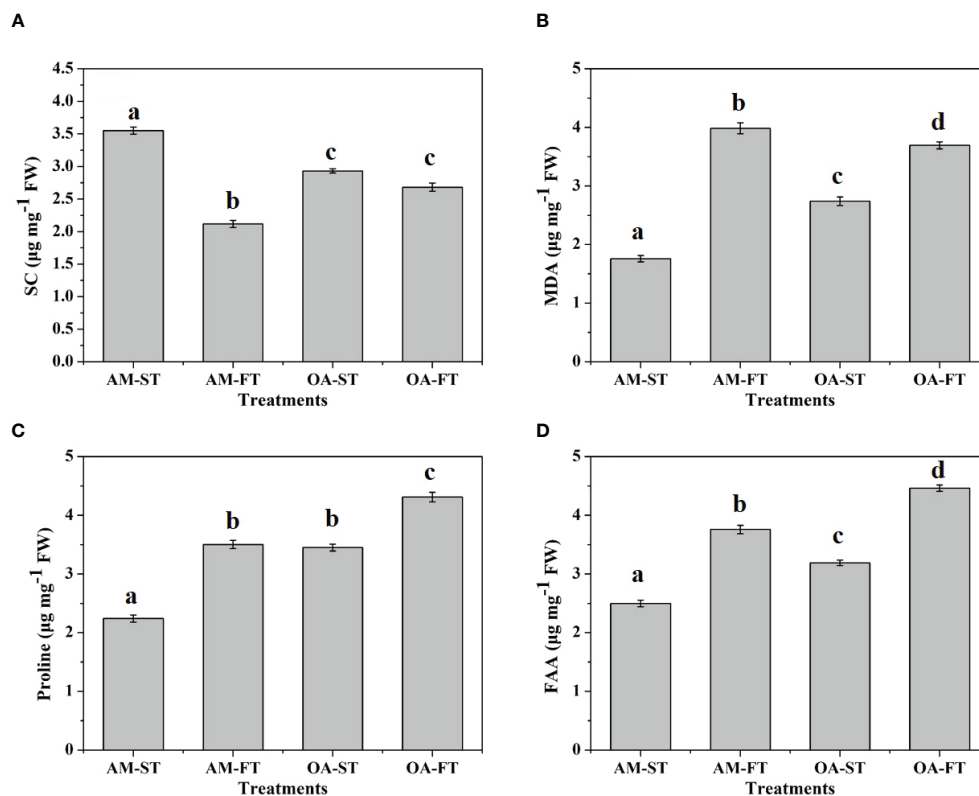
FIGURE 7
Variations in soluble carbohydrate (SC, µg mg^{-1} FW) **(A)**, malondialdehyde (MDA, µg mg^{-1} FW) **(B)**, proline (µg mg^{-1} FW) **(C)** and free amino acids (FAA, µg mg^{-1} FW) **(D)** contents of *Halimeda opuntia* (mean $\pm$ SD, n = 3) in four pCO$_2$ treatments after a 42-day incubation. Significant differences among the treatments are indicated by different uppercase and lowercase letters, respectively (Tukey's test, P<0.05).

2004), the negative effects of elevated pCO$_2$ were mostly attributed to the decreased pH, which disturbs the acid–base balance on the cell surface (Flynn et al., 2012). Subsequently, more metabolic energy has to be expended to resist this interference, resulting in a reduced growth rate (Xu et al., 2017).

The G_{net} of *H. opuntia* was adversely affected by elevated pCO$_2$, which was in keeping with the results of previous studies. Wei et al. (2020a) reported that the G_{net} values of *H. cylindracea* and *H. lacunalis* decrease by 51.78%–62.29% owing to high pCO$_2$ conditions (1,000–1,600 ppmv). Similarly, Campbell et al. (2016)

TABLE 2 Measured seawater parameters of pH (NBS scale), total alkalinity (TA), salinity and temperature, as well as the calculated carbon chemistry of dissolved inorganic carbon (DIC) components (CO$_2$, HCO_3 and CO_3^2) using CO2SYS (Pierrot et al., 2006) in each treatment determined at the end of each light (18:00) and dark (06:00) period during the 42-day experiment.

Treatments		pH$_{NBS}$	Temperature(°C)	TA(µmol kg^{-1})	CO$_2$(µmol kg^{-1})	HCO$_3^-$(µmol kg^{-1})	CO$_3^{2-}$(µmol kg^{-1})	Ω_{Arag}
AM-ST	Day	8.09 ± 0.01	27.1 ± 0.0	2384 ± 16	15.3 ± 0.2	1940.8 ± 3.5	184.2 ± 1.2	3.01 ± 0.19
	Night	8.10 ± 0.01	27.0 ± 0.1	2388 ± 17	14.6 ± 0.1	1898.7 ± 2.5	185.9 ± 0.8	3.03 ± 0.18
AM-FT	Day	8.43 ± 0.01	27.0 ± 0.0	2411 ± 18	5.77 ± 0.3	1601.8 ± 3.1	335.2 ± 0.9	5.47 ± 0.18
	Night	7.72 ± 0.02	27.1 ± 0.1	2384 ± 15	40.2 ± 0.5	2172.2 ± 2.4	88.1 ± 1.3	1.44 ± 0.09
OA-ST	Day	7.71 ± 0.01	27.0 ± 0.1	2406 ± 19	41.5 ± 0.6	2196.0 ± 3.7	87.4 ± 1.1	1.43 ± 0.07
	Night	7.72 ± 0.01	27.0 ± 0.0	2394 ± 17	39.9 ± 0.4	2161.4 ± 2.3	88.3 ± 1.7	1.44 ± 0.06
OA-FT	Day	8.08 ± 0.01	27.0 ± 0.1	2417 ± 10	15.9 ± 0.3	1974.7 ± 1.8	184.0 ± 2.1	3.01 ± 0.14
	Night	7.42 ± 0.02	27.1 ± 0.0	2379 ± 18	86.5 ± 0.7	2243.3 ± 2.7	43.9 ± 0.8	0.72 ± 0.03

Data are the means ± SDs of three measurements.

also demonstrated that the calcification rates of *H. opuntia* and *Halimeda simulans* decline by 15% and 50%, respectively, owing to high pCO_2 concentration (2,400 ppmv). However, other influences were verified for some calcareous organisms, which displayed inconspicuous changes to cope with elevated pCO_2. For instance, Ries et al. (2009) highlighted that the G_{net} of *Halimeda incrassata* only decreases under extremely high pCO_2 (2593 ppmv) conditions, with a Ω_{Arag} value of 0.9. Such differences may be attributed to species-specific acclimation and anti-stress capabilities (Campbell et al., 2016; Wei et al., 2020a, c). The CO_2 enrichment-lowered Ω_{Arag} contributes to the dissolution of micro-anhedral calcareous structures among algal interutricular spaces, especially during dark incubation periods (Andersson et al., 2009). This may cause *Halimeda* to be more susceptible and decomposable than other species (Hofmann et al., 2014). The greatest net dissolution of a calcareous interutricular structure was recorded during a dark period under higher pCO_2 conditions owing to a low Ω_{Arag} and algal respiration (Raven, 2011). This is consistent with previous findings that $CaCO_3$ dissolution occurs in coralline algal species during dark periods, such as in *Corallina pilulifera* incubated at 1,600 ppmv (Gao et al., 1993) and in *Lithothamnion glaciale* grown at 700 ppmv (Budenbender et al., 2011). This addresses the critical influence of Ω_{Arag} status on algal mineralogy (Wei et al., 2020a).

An elevated pCO_2 concentration in surface seawater can promote the photosynthetic processes for some non-calcifying macroalgae, such as *G. lemaneiformis* (Wei et al., 2021), *Pyropia haitanensis* (Chen et al., 2017), *Hizikia fusiformis* (Zou et al., 2011) and *G. chilensis* (Gao et al., 1993), owing to the increased availability of DIC resources. Nevertheless, here, *H. opuntia* showed a negative PSII photochemical efficiency (F_v/F_m) in response to the effects of OA and daily shifts in pCO_2 (pH), which may be caused by the slightly increased the eCAA under high pCO_2 conditions. This suggested that CO_2 concentration may increase in the periplasmic space and lead to enhancement of DIC uptake from environment, although reduced intracellular Ci (DIC) pools (Raven et al., 2012) and poorly passive CO_2 diffusion (Elzenga and Prins, 1989; Miedema and Prins, 1991). Similar conclusions have been made for other *Halimeda* species. Sinutok et al. (2012) found notable declines (50%–70%) of F_v/F_m values in *Halimeda macroloba* and *H. cylindracea* after a 35-day exposure to elevated pCO_2 condition (1,200 ppmv, Ω_{Arag}: 1.97 ± 0.02). Concurrently, a decline in the Chl-*a* contents under static/fluctuating low pH conditions indicated the down-regulation of Chl accumulation or pigment degradation, whereas there were limited effects of elevated pCO_2 on Chl-*b* and carotenoid contents. The lack of changes in photosynthetic performance and pigment contents in *H. opuntia* under fluctuating OA condition was most probably owing to 1) their high tolerance and increased retention of phenotypic plasticity to the dramatic variations in pCO_2 (pH), because they regularly experience daily fluctuations in pH in the coastal regions; and/or 2) a higher daytime pH,

which provides a period of suitable conditions for macroalgal photosynthesis (Cornwall et al., 2013).

An elevated/fluctuating pCO_2 is predicted to modulate TC_{org} and TN accumulations in *H. opuntia* tissues. The changes in TC_{org} and TN contents may be due to variations in the characterizations of enzymatic activities (Wei et al., 2021). At static higher pCO_2 levels, the eCAA in chloroplast slightly increased (although there was no statistically significant difference), and this may accelerate the interconversion between CO_2 and HCO_3^-, guaranteeing soluble carbohydrate synthesis at the carboxylation site (Vidal-Dupiol et al., 2013). Meanwhile, the SC synthesis was enhanced by the positive effects of eCAA activity, which played a role in an improvement in the irradiance harvesting capacity and up-regulation of the photosynthetic electron transport chain (Van Oijen et al., 2004). Moreover, a discrepancy in the average NRA was negatively influenced by diurnal fluctuating pCO_2, leading to a noticeable decrease in N accumulations in algal tissues (Figure 6). When NRA decreases, variations in elevated pCO_2 can promote the ammonium to nitrate conversion process, leading to the formation of glutamine and thereby inhibiting NRA (Stitt and Krapp, 1999). Such a response would demand less energy for the formation of ammonium than nitrate and allow this macroalga to allocate more energy for regulating eCAA and C acquisition (Losada and Guerrero, 1979; Syrett, 1981). These findings indicate that the elevated pCO_2 caused modifications in algal C vs. N metabolism, and the increased variability in pCO_2 amplified these influences, which was confirmed by eCAA and NRA driven activities.

The MDA content is used to evaluate lipid peroxidation levels in cell systems (Hodges et al., 1999). Under elevated pCO_2 conditions, *H. opuntia* displayed greater oxidative lipid degradation associated with higher MDA contents, and this adverse physiological performance was amplified in both fluctuating pCO_2 treatments. This was in agreement with the decreased algal growth and lower photosynthetic activity (F_v/F_m) levels. The SC synthesis declined sharply under elevated and fluctuating pCO_2 conditions due to the depression of PSII activities (Wei et al., 2021), which would in turn down-regulate the irradiance harvesting capacity and photosynthetic activities (Van Oijen et al., 2004). Therefore, it is essential for *H. opuntia* to undergo appropriate adjustments to cope with the elevated pCO_2 pressure (Wei et al., 2020a; Wei et al., 2020c; Wei et al., 2021). Our findings indicate that soluble organic molecules (FAAs and proline) are highly secreted and likely linked to protecting the integrity of cellular structures (Sun et al., 2013; Chen et al., 2018; Wei et al., 2020a; Wei et al., 2020c). Thus, as the experiment progressed, greater contents of proline and FAA were obtained in OA, and these effects were strengthened under the two fluctuating pCO_2 conditions, which played a positive role in maintaining the photosynthetic system's function and in protecting membrane integrity (Xiong et al., 2002). This explanation is corroborated by a previous analysis by Wei

et al., (2020a); Wei et al., 2021), who suggested that these modifications give rise to the internal re-partitioning of C and N in *Halimeda* tissues.

In summary, this study attempted to mimic *in situ* pH (pCO$_2$) changes, and it demonstrated that a static elevated pCO$_2$ level has adverse effects on the growth, calcification, photosynthesis and other C vs. N metabolic activities of *H. opuntia*. Moreover, diurnal fluctuations in pCO$_2$ amplified these negative influences of OA, especially during the night time. Under the stress of elevated and/or fluctuating pCO$_2$, higher MDA contents were obtained, which indicates that the cellular membranes were damaged. This generated a dynamic balance in *H. opuntia* incubated under environmental stress conditions, and it is reasonable to suggest that high contents of proline and FAA, in combination with related-enzymatic activities, play positive roles in protecting cellular structures and mitigating adverse influences. The results of the present study increase our understanding of the biological consequences of pH (pCO$_2$) variability on specific marine calcifiers and their physiological plasticity under future OA conditions.

Data availability statement

The original contributions presented in the study are included in the article/supplementary material. Further inquiries can be directed to the corresponding authors.

Author contributions

The authors thank all the staff, and particularly LL who conceived and designed the experiments. ZW performed the experiments and wrote the paper. FY analyzed the data, and YZ contributed materials and analysis tools. LL agrees to serve as the author responsible for contact and communication. All authors contributed to the article and approved the submitted version.

Conflict of interest

The authors declare that the research was conducted in the absence of any commercial or financial relationships that could be construed as a potential conflict of interest.

Publisher's note

All claims expressed in this article are solely those of the authors and do not necessarily represent those of their affiliated organizations, or those of the publisher, the editors and the reviewers. Any product that may be evaluated in this article, or claim that may be made by its manufacturer, is not guaranteed or endorsed by the publisher.

References

Andersson, A. J., Kuffner, I. B., Mackenzie, F. T., Jokiel, P. L., Rodgers, K. S., and Tan, A. (2009). Net loss of CaCO3 from coral reef communities due to human induced seawater acidification. *Biogeosciences* 6, 2163–2182. doi: 10.5194/bg-6-1811-2009

Bao, M., Wang, J., Xu, T., Wu, H., Li, H., and Xu, J. (2019). Rising CO2 levels alter the responses of the red macroalga pyropia yezoensis under light stress. *Aquaculture* 501, 325–330. doi: 10.1016/j.aquaculture.2018.11.011

Beach, K., Walters, L., Vroom, P., Smith, C., Coyer, J., and Hunter, C. (2003). Variability in the ecophysiology of halimeda spp. (Chlorophyta, bryopsidales) on conch reef, Florida keys, USA. *J. Phycol.* 39 (4), 633–643.

Budenbender, J., Riebesell, U., and Form, A. (2011). Calcification of the Arctic coralline red algae lithothamnion glaciale in response to elevated CO2. *Mar. Ecol.-Prog. Ser.* 441, 79–87. doi: 10.3354/meps09405

Caldeira, K., and Wickett, M. E. (2003). Oceanography: anthropogenic carbon and ocean pH. *Nature.* 425 (6956), 365. doi: 10.1038/425365a

Caldeira, K., and Wickett, M. E. (2005). Ocean model predictions of chemistry changes from carbon dioxide emissions to the atmosphere and ocean. *J. Geophys. Res.-Oceans.* 110 (C9), C09S04. doi: 10.1029/2004JC002671

Campbell, J. E., Fisch, J., Langdon, C., and Paul, V. J. (2016). Increased temperature mitigates the effects of ocean acidification in calcified green algae (Halimeda spp.). *Coral Reefs.* 35, 357–368. doi: 10.1007/s00338-015-1377-9

Chen, B., Zou, D., Du, H., and Ji, W. (2018). Carbon and nitrogen accumulation in the economic seaweed gracilaria lemaneiformis affected by ocean acidification and increasing temperature. *Aquaculture.* 482, 176–182. doi: 10.1016/j.aquaculture.2017.09.042

Chen, B., Zou, D., and Yang, Y. (2017). Increased iron availability resulting from increased CO2 enhances carbon and nitrogen metabolism in the economical marine red macroalga pyropia haitanensis (Rhodophyta). *Chemosphere* 173, 444–451. doi: 10.1016/j.chemosphere.2017.01.073

Cornwall, C. E., Hepburn, C. D., McGraw, C. M., Currie, K. I., Pilditch, C. A., Hunter, K. A., et al. (2013). Diurnal fluctuations in seawater pH influence the response of a calcifying macroalga to ocean acidification. *Proc. R. Soc B-Biol. Sci.* 280 (1772), 20132201. doi: 10.1098/rspb.2013.2201

Dickson, A. G., Sabine, C. L., and Christian, J. R. (2007). *Guide to best practices for ocean CO2 measurements, in PICES special publication* (Sidney, Canada: North Pacific Marine Science Organization), 67–81.

Dufault, A. M., Cumbo, V. R., Fan, T. Y., and Edmunds, P. J. (2012). Effects of diurnally oscillating pCO2 on the calcification and survival of coral recruits. *Proc. R. Soc B-Biol. Sci.* 279, 2951–2958. doi: 10.1098/rspb.2011.2545

Egilsdottir, H., Noisette, F., Noël, L. M. L. J., Olafsson, J., and Martin, S. (2013). Effects of pCO2 on physiology and skeletal mineralogy in a tidal pool coralline alga corallina elongata. *Mar. Biol.* 160, 2103–2112. doi: 10.1007/s00227-012-2090-7

Elzenga, J. T. M., and Prins, H. B. A. (1989). Light-induced polar pH changes in leaves of elodea canadensis. i. effects of carbon concentration and light intensity. *Plant Physiol.* 91, 62–67. doi: 10.1104/pp.91.1.62

Flynn, K. J., Blackford, J. C., Baird, M. E., Raven, J. A., Clark, D. R., Beardall, J., et al. (2012). Changes in pH at the exterior surface of plankton with ocean acidification. *Nat. Clim. Change* 2, 510–513. doi: 10.1038/nclimate1489

Friedlingstein, P., Jones, M., O'Sullivan, M. W., Andrew, R. M., Bakker, D. C. E., Hauck, J., et al. (2022). Global carbon budget 2021. *Earth Syst. Sci. Data* 14, 1917–2005. doi: 10.5194/essd-14-1917-2022

Gao, K., Aruga, Y., Asada, K., and Kiyohara, M. (1993). Influence of enhanced CO2 on growth and photosynthesis of the red algae gracilaria sp. and g. chilensis. *J. Appl. Phycol.* 5, 563–571. doi: 10.1007/BF02184635

Gao, G., Clare, A. S., Rose, C., and Caldwell, G. S. (2018). Ulva rigida in the future ocean: potential for carbon capture, bioremediation, and biomethane production. *GCB. Bioenergy.* 10, 39–51. doi: 10.1111/gcbb.12465

Gao, G., Liu, Y., Li, X., Feng, Z., Xu, Z., Wu, H., et al. (2017). Expected CO2-induced ocean acidification modulates copper toxicity in the green tide alga ulva prolifera. *Environ. Exp. Bot.* 135, 63–72. doi: 10.1016/j.envexpbot.2016.12.007

Gattuso, J. P., Magnan, A., Billé, R., Cheung, W. W. L., Howes, E. L., Joos, F., et al. (2015). Contrasting futures for ocean and society from different anthropogenic CO2 emissions scenarios. *Science.* 349 (6243), 45–55.

Hillis, L. W. (2001). The calcareous reef alga halimeda (Chlorophyta, byropsidales): a cretaceous genus that diversified in the Cenozoic. *Paleogeogr. Paleoclimatol. Paleoecol.* 166 (1–2), 89–100. doi: 10.1016/S0031-0182(00)00203-0

Hodges, D. M., DeLong, J. M., Forney, C. F., and Prange, R. K. (1999). Improving the thiobarbituric acid-reactive-substances assay for estimating lipid peroxidation in plant tissues containing anthocyanin and other interfering compounds. *Planta.* 207, 604–611. doi: 10.1007/s004250050524

Hofmann, L. C., Heiden, J., Bischof, K., and Teichberg, M. (2014). Nutrient availability affects the response of the calcifying chlorophyte halimeda opuntia (L.) J.V. lamouroux to low pH. *Planta.* 239 (1), 231–242.

Hurd, C. L., Cornwall, C. E., Currie, K. I., Hepburn, C. D., McGraw, C. M., Hunter, K. A., et al. (2011). Metabolically-induced pH fluctuations by some coastal calcifiers exceed projected 22nd century ocean acidification: a mechanism for differential susceptibility? *Glob. Change Biol.* 17 (10), 3254–3262. doi: 10.1111/j.1365-2486.2011.02473.x

Jury, C. P., Whitehead, R. F., and Szmant, A. M. (2010). Effects of variations in carbonate chemistry on the calcification rates of madracis auretenra (= madracis mirabilis sensu well: bicarbonate concentrations best predict calcification rates). *Glob. Change Biol.* 16 (5), 1632–1644. doi: 10.1111/j.1365-2486.2009.02057.x

Kochert, G. (1978). "Protein determination by dye binding," in *Handbook of phycological methods: Physiological and biochemical methods.* Eds. J. A. Hellebust and J. S. Craigie (Cambridge, UK: Cambridge University Press), 92–93.

Kroeker, K. J., Kordas, R. L., Crim, R. N., and Singh, G. G. (2010). Meta-analysis reveals negative yet variable effects of ocean acidification on marine organisms. *Ecol. Lett.* 13, 1419–1434. doi: 10.1111/j.1461-0248.2010.01518.x

Losada, M., and Guerrero, M. G. (1979). "The photosynthetic reduction of nitrate and its regulation," in *Photosynthesis in relation to model systems* (Amsterdam: Elsevier), 365–408.

Martin, S., and Gattuso, J. P. (2009). Response of Mediterranean coralline algae to ocean acidification and elevated temperature. *Glob. Change Biol.* 15 (8), 2089–2100. doi: 10.1111/j.1365-2486.2009.01874.x

Masson-Delmotte, V., Zhai, P., Pirani, A., Connors, S. L., Péan, C., Berger, S., et al., eds. (2021). IPCC, 2021: Climate Change 2021: The physical science basis. Contribution of working group I to the sixth assessment report of the intergovernmental panel on climate change. Cambridge University Press.

Mercado, J. M., Javier, F., Gordillo, L., Niell, F. X., and Figueroa, F. L. (1999). Effects of different levels of CO2 on photosynthesis and cell components of the red alga porphyra leucosticta. *J. Appl. Phycol.* 11 (5), 455–461. doi: 10.1023/A:1008194223558

Miedema, H., and Prins, H. B. A. (1991). pH-dependent proton permeability of the plasma membrane is a regulating mechanism of polar transport through the submerged leaves of potamogeton lucens. *Can. J. Bot.-Rev. Can. Bot.* 69, 1116–1122. doi: 10.1139/b91-143

Milliman, J. D. (1993). Production and accumulation of calcium carbonate in the ocean: budget of a nonsteady state. *Glob. Biogeochem Cycle* 7 (4), 927–957. doi: 10.1029/93GB02524

Olischläger, M., and Wiencke, C. (2013). Ocean acidification alleviates low-temperature effects on growth and photosynthesis of the red alga neosiphonia harveyi (Rhodophyta). *J. Exp. Bot.* 64, 5587–5597. doi: 10.1093/jxb/ert329

Peach, K. E., Koch, M. S., Blackwelder, P. L., and Manfrino, C. (2017). Calcification and photophysiology responses to elevated pCO2 in six halimeda species from contrasting irradiance environments on little Cayman island reefs. *J. Exp. Mar. Biol. Ecol.* 486, 114–126. doi: 10.1016/j.jembe.2016.09.008

Pierrot, D., Lewis, E., and Wallace, D. W. R. (2006). "MS excel program developed for CO2 systems calculations: ORNL/CDIAC-105a," in *Carbon dioxide information analysis center oak ridge national laboratory* (Tennessee: U.S. Department of Energy, Oak Ridge).

Poole, L. J., and Raven, J. A. (1997). The biology of enteromorpha. *Prog. Phycol. Res.* 12, 1–148.

Qu, L., Xu, J., Sun, J., Li, X., and Gao, K. (2017). Diurnal pH fluctuations of seawater influence the responses of an economic red macroalga gracilaria lemaneiformis to future CO2-induced seawater acidification. *Aquaculture.* 473, 383–388. doi: 10.1016/j.aquaculture.2017.03.001

Ragazzola, F., Foster, L. C., Form, A., Anderson, P. S. L., Hansteen, T. H., and Fietzke, J. (2012). Ocean acidification weakens the structural integrity of coralline algae. *Glob. Change Biol.* 18, 2804–2812. doi: 10.1111/j.1365-2486.2012.02756.x

Rautenberger, R., Fernández, P. A., Strittmatter, M., Heesch, S., Cornwall, C. E., Hurd, C. L., et al. (2015). Saturating light and not increased carbon dioxide under ocean acidification drives photosynthesis and growth in ulva rigida (Chlorophyta). *Ecol. Evol.* 5 (4), 874–888. doi: 10.1002/ece3.1382

Raven, J. A. (2011). Effects on marine algae of changed seawater chemistry with increasing atmospheric CO2. *Biol. Environ.-Proc. R. Irish Acad.* 111B, 1–17. doi: 10.3318/bioe.2011.01

Raven, J. A., Giordano, M., Beardall, J., and Maberly, S. C. (2012). Algal evolution in relation to atmospheric CO2: carboxylases, carbon concentrating mechanisms and carbon oxidation cycles. *Philos. Trans. R. Soc B-Biol. Sci.* 367, 493–507. doi: 10.1098/rstb.2011.0212

Reusch, T. B. H., and Boyd, P. W. (2013). Experimental evolution meets marine phytoplankton. *Evolution.* 67 (7), 1849–1859. doi: 10.1111/evo.12035

Ries, J. B., Cohen, A. L., and McCorkle, D. C. (2009). Marine calcifiers exhibit mixed responses to CO2-induced ocean acidification. *Geology* 37, 1131–1134. doi: 10.1130/G30210A.1

Ritchie, R. J. (2008). Universal chlorophyll equations for estimating chlorophylls a, b, c, and d and total chlorophylls in natural assemblages of photosynthetic organisms using acetone, methanol, or ethanol solvents. *Photosynthetica.* 46, 115–126. doi: 10.1007/s11099-008-0019-7

Shan, D., Huang, J., Yang, Y., Guo, Y., Wu, C., Yang, G., et al. (2007). Cotton GhDREB1 increases plant tolerance to low temperature and is negatively regulated by gibberellic acid. *New Phytol.* 176, 70–81. doi: 10.1111/j.1469-8137.2007.02160.x

Sinutok, S., Hill, R., Doblin, M. A., Kuhl, M., and Ralph, P. J. (2012). Microenvironmental changes support evidence of photosynthesis and calcification inhibition in halimeda under ocean acidification and warming. *Coral Reefs.* 31, 1201–1213. doi: 10.1007/s00338-012-0952-6

Stitt, M., and Krapp, A. (1999). The interaction between elevated carbon dioxide and nitrogen nutrition: the physiological and molecular background. *Plant Cell Environ.* 22, 583–621. doi: 10.1046/j.1365-3040.1999.00386.x

Sun, Y., Wang, B., Jin, S., Qu, X., Li, Y., and Hou, B. (2013). Ectopic expression of arabidopsis glycosyltransferase UGT85A5 enhances salt stress tolerance in tobacco. *PloS One* 8 (3), e59924. doi: 10.1371/journal.pone.0059924

Syrett, P. J. (1981). Nitrogen metabolism of microalgae. *Can. J. Fish Aquat Sci.* 210, 182–210. doi: 10.1016/0044-8486(81)90166-6

Teichberg, M., Fricke, A., and Bischol, K. (2013). Increased physiological performance of the calcifying green macroalga halimeda opuntia in response to experimental nutrient enrichment on a Caribbean coral reef. *Aquat. Bot.* 104, 25–33. doi: 10.1016/j.aquabot.2012.09.010

Van Oijen, T., Van Leeuwe, M. A., Gieskes, W. W. C., and De Baar, H. J. W. (2004). Effects of iron limitation on photosynthesis and carbohydrate metabolism in the Antarctic diatom. *Eur. J. Phycol.* 39, 161–171. doi: 10.1080/0967026042000202127

Vidal-Dupiol, J., Zoccola, D., Tambutte, E., Grunau, C., Cosseau, C., Smith, K. M., et al. (2013). Genes related to ion-transport and energy production are unregulated in response to CO2-driven pH decrease in corals: new insights from transcriptome analysis. *PloS One* 8 (3), e58652. doi: 10.1371/journal.pone.0058652

Vogel, N., Fabricius, K. E., Strahl, J., Noonan, S. H. C., Wild, C., and Uthicke, S. (2015). Calcareous green alga halimeda tolerates ocean acidification conditions at tropical carbon dioxide seeps. *Limnol. Oceanogr.* 60, 263–275. doi: 10.1002/lno.10021

Wei, Z., Long, C., Yang, F., Long, L., Huo, Y., Ding, D., et al. (2020a). Increased irradiance availability mitigates the physiological performance of species of the

calcifying green macroalga halimeda in response to ocean acidification. *Algal Res.* 48, 101906. doi: 10.1016/j.algal.2020.101906

Wei, Z., Long, C., Yang, F., Long, L., Mo, J., Hu, Q., et al. (2020b). Effects of plant growth regulators on physiological performances of three calcifying green macroalgae halimeda species (Bryopsidales, chlorophyta). *Aquat. Bot.* 161, 103186. doi: 10.1016/j.aquabot.2019.103186

Wei, Z., Mo, J., Huang, R., Hu, Q., Long, C., Ding, D., et al. (2020c). Physiological performance of three calcifying green macroalgae halimeda species in response to altered seawater temperatures. *Acta Oceanol. Sin.* 39 (02), 89–100. doi: 10.1007/s13131-019-1471-3

Wei, Z., Zhang, Y., Yang, F., Liang, J., and Long, L. (2021). Increased light availability modulates carbon and nitrogen accumulation in the macroalga gracilariopsis lemaneiformis (Rhodophyta) in response to ocean acidification. *Environ. Exp. Bot.* 187, 104492. doi: 10.1016/j.envexpbot.2021.104492

Wizemann, A., Meyer, F. W., Hofmann, L. C., Wild, C., and Westphal, H. (2015). Ocean acidification alters the calcareous microstructure of the green macro-alga halimeda opuntia. *Coral Reefs.* 34, 941–954. doi: 10.1007/s00338-015-1288-9

Xiong, L., Schumaker, K. S., and Zhu, J. (2002). Cell signaling during cold, drought, and salt stress. *Plant Cell.* 14, S165–S183. doi: 10.1105/tpc.000596

Xu, Z., Gao, G., Xu, J., and Wu, H. (2017). Physiological response of a golden tide alga (Sargassum muticum) to the interaction of ocean acidification and phosphorus enrichment. *Biogeosciences.* 14, 671–681. doi: 10.5194/bg-14-671-2017

Yildiz, G., Hofmann, L. C., Bischof, K., and Dere, S. (2013). Ultraviolet radiation modulates the physiological responses of the calcified rhodophyte corallina officinalis to elevated CO2. *Bot. Mar.* 56, 161–168. doi: 10.1515/bot-2012-0216

Zou, D., Gao, K., and Luo, H. (2011). Short- and long term effects of elevated CO2 on photosynthesis and respiration in the marine macroalga hizikia fusiformis (Sargassaceae, phaeophyta) grown at low and high n supplies. *J. Phycol.* 47, 87–97. doi: 10.1111/j.1529-8817.2010.00929.x

Zou, D., Xia, J., and Yang, Y. (2004). Photosynthetic use of exogenous inorganic carbon in the agarophyte gracilaria lemaneiformis (Rhodophyta). *Aquaculture.* 237, 421–431. doi: 10.1016/j.aquaculture.2004.04.020